PHYSICAL REVIEW D **90,** 114012 (2014)

Double spin asymmetries through QCD instantons

Yachao Qian and Ismail Zahed

Department of Physics and Astronomy, Stony Brook University, Stony Brook, New York 11794-3800, USA

(Received 18 August 2014; published 8 December 2014)

We revisit the large instanton contribution to the gluon Pauli form factor of the constituent quark noted by Kochelev. We check that it contributes sizably to the single spin asymmetry in polarized $p_\uparrow p \to \pi X$. We use it to predict a large double spin asymmetry in doubly polarized $p_\uparrow p_\uparrow \to \pi\pi X$.

DOI: 10.1103/PhysRevD.90.114012 PACS numbers: 13.88.+e, 11.30.Rd, 12.38.-t

I. INTRODUCTION

The QCD vacuum is dominated by large instanton and anti-instanton fluctuations in the infrared that are largely responsible for the spontaneous breaking of chiral symmetry and the anomalously large η' mass [1,2]. QCD instantons may contribute substantially to small angle hadron-hadron scattering [3–7] and possibly gluon saturation at HERA [8,9], as evidenced by recent lattice investigations [10,11].

A number of semi-inclusive DIS experiments carried by the CLAS, HERMES and COMPASS collaborations [12–17], and more recently with polarized protons on protons by the STAR and PHENIX collaborations [18–20], have revealed large spin asymmetries in polarized lepton-hadron and hadron-hadron collisions at collider energies. T-odd effects may be important in these processes.

Perturbative QCD does not quantitatively explain such large asymmetries because it does not support T-odd contributions. The latter can be encoded into elementary nonperturbative mechanisms such as the Sivers effect [21,22] and the Collins effect [23–26]. Many efforts have been made to give a quantitative description of these nonperturbative mechanisms in spectator models [27–32], MIT bag models [33,34], and constituent quark models [35–37]. Nonperturbative QCD instantons offer another mechanism to explain these large spin asymmetries as discussed by Kochelev and others [38–41]. In [38] a particularly large Pauli form factor was noted, with an important contribution to the single spin asymmetry (SSA) in polarized proton on proton scattering. In this note we point out that it contributes significantly to doubly polarized proton on proton scattering.

The organization of the paper is as follows: In Sec. II we review the emergence of a large Pauli form factor on a constituent quark in the QCD vacuum. In Sec. III we assess its effect on the transverse SSA in $p_\uparrow p \to \pi^{\pm,0} X$ following a recent argument in [42]. The effect is comparable in magnitude to the one discussed in [40,41]. In Sec. IV we show that it gives a substantial contribution to the double spin asymmetry (DSA) in semi-inclusive $p_\uparrow p_\uparrow \to \pi\pi X$. Our conclusions follow in Sec. V.

II. EFFECTIVE PAULI FORM FACTOR

The QCD vacuum is a random ensemble of instantons and anti-instantons interacting via the exchange of perturbative gluons and quasizero modes of light quarks and antiquarks. In the dilute instanton approximation, a typical effective vertex with quarks and gluons attached to an instanton is shown in Fig. 1. The corresponding effective vertex is given by [43–45],

$$\mathcal{L} = \int \prod_q \left[m_q\rho - 2\pi^2\rho^3 \bar{q}_R \left(1 + \frac{i}{4}\tau^a \bar{\eta}^a_{\mu\nu}\sigma_{\mu\nu}\right) q_L \right] \times \exp\left(-\frac{2\pi^2}{g_s}\rho^2 \bar{\eta}^b_{\gamma\delta} G^b_{\gamma\delta} F_g(\rho Q)\right) d_0(\rho)\frac{d\rho}{\rho^5} d\bar{\sigma} + (L \leftrightarrow R) \tag{1}$$

where $d\bar{\sigma}$ is the integration over the instanton orientation in color space and $\sigma_{\mu\nu} = [\gamma_\mu, \gamma_\nu]/2$. Here ρ is the instanton size, g_s is the $SU(3)$ coupling constant, $\bar{\eta}^a_{\mu\nu}$ is the 't Hooft symbol and $d_0(\rho)$ is the density of instanton. The incoming and outgoing quarks have small momenta p ($\rho p \ll 1$) and Q is the momentum transferred by the inserted gluon with a form factor

$$F_g(x) \equiv \frac{4}{x^2} - 2K_2(x) \xrightarrow{x\to 0} 1. \tag{2}$$

By expanding Eq. (1) to leading order in the inserted gluon field of $G^b_{\gamma\delta}$ and integrating over the color indices, we obtain

$$\frac{i}{g_s}F_g(\rho Q)\int \pi^4\rho^4 \frac{\bar{q}_R t^a \sigma_{\mu\nu} q_L}{m_q^*} G^a_{\mu\nu} \times \left(\prod_q (\rho m_q^*) d_0(\rho)\frac{d\rho}{\rho^5}\right) = \frac{i}{g_s}F_g(\rho Q)\int d\rho \pi^4\rho^4 n(\rho)\frac{\bar{q}_R t^a \sigma_{\mu\nu} q_L}{m_q^*} G^a_{\mu\nu} \tag{3}$$

where $n(\rho)$ is the effective instanton density and m_q^* is the effective quark mass. In the dilute instanton approximation [46]

$$n(\rho) = n_I \delta(\rho - \rho_c) \tag{4}$$

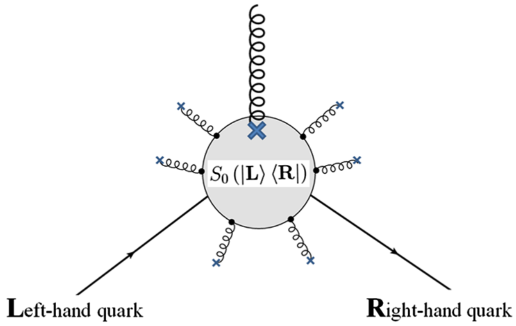

FIG. 1 (color online). Effective quark-gluon vertex in the instanton vacuum.

where ρ_c is the average size of the instanton. Hence the induced instanton effective quark-gluon vertex

$$\frac{i}{g_s} F_g(\rho_c Q)\pi^4 (n_I \rho_c^4) \frac{\bar{q}_R t^a \sigma_{\mu\nu} q_L}{m_q^*} G^a_{\mu\nu} \tag{5}$$

as illustrated in Fig. 1. In momentum space, the effective vertex is M^a_μ and reads

$$M^a_\mu = \gamma_\mu t^a - \frac{2}{g_s^2} F_g(\rho_c Q)\pi^4 (n_I \rho_c^4) \frac{t^a \sigma_{\mu\nu}}{m_q^*} q^\nu \tag{6}$$

after analytical continuation to Minkowski Space. Equation (5) yields an anomalously large quark chromomagnetic moment [45]

$$\mu_a = -\frac{2 n_I \pi^4 \rho_c^4}{g_s^2}. \tag{7}$$

III. SINGLE SPIN ASYMMETRIES

A. SSA: estimate

To calibrate the effects of Eq. (6) on the double spin asymmetries, we revisit its contribution to the SSA on semi-inclusive and polarized $p_\uparrow p \to \pi^{\pm,0} X$ experiments. This effect was recently discussed in [42], so we will be brief. In going through an instanton, the chirality of the light quark can be flipped. Using the Pauli form factor discussed in Sec. II, the SSA follows from the diagrams of Fig. 2. As noted in [42], the leading diagram contributing to the SSA is displayed in Fig. 3. Note that Fig. 3 is of the same order in g_s as the zeroth order diagram in Fig. 2, since the chirality-flip effective vertex [Eq. (6)] is semiclassical and of order $1/g_s^2$. The zeroth order differential cross section reads

$$d^{(0)}\sigma \sim \frac{64 g_s^4}{|p_1 - k_1|^4} [(k_1 \cdot p_2)(k_2 \cdot p_1) + (k_1 \cdot k_2)(p_1 \cdot p_2)]. \tag{8}$$

The first order differential cross section for the chirality flip reads [47]

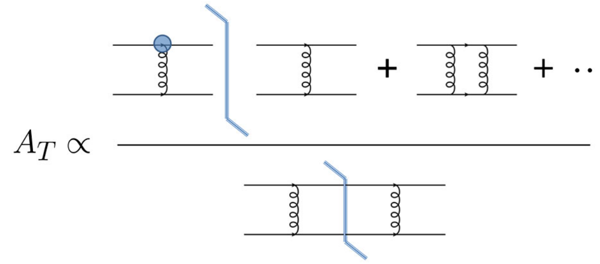

FIG. 2 (color online). Schematically diagrammatic contributions to the SSA through the Pauli form factor [42].

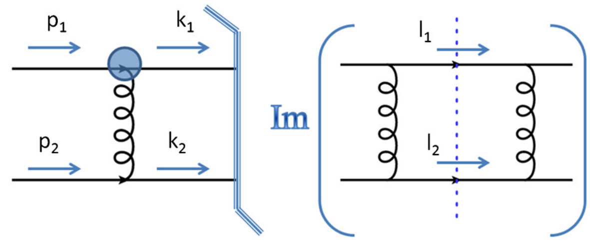

FIG. 3 (color online). Leading diagrammatic contribution to the SSA through the Pauli form factor.

$$d^{(1)}\sigma \sim i \frac{g_s^6}{(k_1 - p_1)^2} \frac{1}{16\pi} \frac{(4\pi)^\epsilon}{\Gamma(1-\epsilon)} \frac{\mu^{2\epsilon}}{s^\epsilon} \int_0^1 dy [y(1-y)]^{-\epsilon} \times \int_0^{2\pi} \frac{d\phi_l}{2\pi} \frac{1}{(l_1 - k_1)^2} \frac{1}{(p_1 - l_1)^2} \mathcal{G}(\Omega) \tag{9}$$

where $y = (1 + \cos\theta_l)/2$, $\pm\theta_l$ is the longitudinal angle of $l_{1/2}$ and

$$\mathcal{G}(\Omega) \equiv \mathrm{tr}[(M^a_\mu)^{(1)} \not{p}_1 \gamma_5 \not{s} \gamma_\nu t^b \not{l}_1 \gamma_\rho t^c \not{k}_1] \mathrm{tr}[\gamma^\mu t_a \not{p}_2 \gamma^\nu t_b \not{l}_2 \gamma^\rho t_c \not{k}_2]. \tag{10}$$

From Sec. II

$$(M^a_\mu)^{(1)} = -\frac{t^a}{g_s^2} \frac{F_g(\rho Q)\pi^4 (n_I \rho_c^4)}{m_q^*} [\gamma_\mu (\not{k}_1 - \not{p}_1) + (\not{p}_1 - \not{k}_1)\gamma_\mu]. \tag{11}$$

To simplify the analysis and compare to existing semi-inclusive data, we use the kinematics

$$\begin{aligned} p_{1/2} &= \frac{\sqrt{s}}{2}(1, 0, 0, \pm 1) \\ k_{1/2} &= \frac{\sqrt{s}}{2}(1, \pm\sin\theta\sin\phi, \pm\sin\theta\cos\phi, \pm\cos\theta) \\ s &= (0, 0, s^\perp, 0) \end{aligned} \tag{12}$$

where $\sqrt{\tilde{s}}$ is the total energy of the colliding "partons." It is simple to show that $d^{(1)}\sigma \sim \vec{k}_1 \cdot (\vec{p}_1 \times \vec{s}) \sim \sqrt{\tilde{s}} s^\perp k_1^\perp \sin\phi$, which results in SSA. For simplicity, we calculate the first differential cross section $d^{(1)}\sigma$ with $\phi = \pi/2$, where the transverse momentum of the outgoing particle lies along the x axis. Straightforward algebra yields

$$d^{(1)}\sigma \sim s^\perp k_1^\perp \frac{2g_s^4}{3\pi} \frac{\Gamma(-\epsilon)}{\Gamma(2-2\epsilon)\Gamma(1-\epsilon)} \csc^2(\theta)(4\pi)^\epsilon \frac{\mu^{2\epsilon}}{s^\epsilon} \frac{F_g(\rho_c Q)\pi^4(n_I\rho_c^4)}{m_q^*} \times \left[25\epsilon - 12 + \cos\theta(\epsilon(9+2\epsilon)-4)\,{}_2F_1\left(1, 1-\epsilon, 1-2\epsilon, \sec^2\frac{\theta}{2}\right) + \epsilon(1-\cos\theta)\,{}_2F_1\left(2, 1-\epsilon, 1-2\epsilon, \sec^2\frac{\theta}{2}\right)\right] \tag{13}$$

where ${}_2F(a,b,c;y)$ is a hypergeometric function. We note that $|{}_2F_1(1,1,1;y)|$ is much larger than $|{}_2F_1^{(0,1,0,0)}(1,1,1;y)|$ and $|{}_2F_1^{(0,0,1,0)}(1,1,1;y)|$ for $y \sim 1$. Therefore

$$d^{(1)}\sigma \sim s^\perp k_1^\perp \frac{2g_s^4}{3\pi} \frac{F_g(\rho_c Q)\pi^4(n_I\rho_c^4)}{m_q^*} \csc^4\left(\frac{\theta}{2}\right)(3+\cos\theta) \times \left(-\frac{1}{\epsilon} + 2\gamma_{\mathrm{E}} + \ln\left(\frac{\tilde{s}}{4\pi\mu^2}\right)\right). \tag{14}$$

The divergence in (14) stems from the exchange of soft gluons in the box diagram. In [42] it was regulated using a constituent gluon mass m_g. For $\theta_l \sim 0$, $\vec{l}_1$ is parallel to $\vec{p}_1$, and this collinear divergence could be regulated by restricting $-(l_1 - p_1)^2 > m_g^2$ or equivalently setting $y_{\max} \sim 1 - cm_g^2/\tilde{s}$ with c being an arbitrary constant of order 1. This regularization amounts to the substitution

$$\int_0^1 dy \longrightarrow \left(\int_0^{\frac{1+\cos\theta}{2} - c\frac{m_g^2}{\tilde{s}}} + \int_{\frac{1+\cos\theta}{2} + c\frac{m_g^2}{\tilde{s}}}^{1-c\frac{m_g^2}{\tilde{s}}}\right) dy \tag{15}$$

in Eq. (9), where we have also regulated the collinear divergence when $\vec{l}_1$ is parallel to $\vec{k}_1$. Thus

$$\left(-\frac{1}{\epsilon} + 2\gamma_{\mathrm{E}} + \ln\left(\frac{\tilde{s}}{4\pi\mu^2}\right)\right) \longrightarrow \ln\left(c\frac{\tilde{s}}{m_g^2}\right) + \ln\left(\frac{1-\cos\theta}{1+\cos\theta}\right). \tag{16}$$

The regulated SSA is now given by

$$A_T^{\sin\phi} \approx \frac{d^{(1)}\sigma}{d^{(0)}\sigma} = s^\perp k_1^\perp \frac{F_g(\rho_c Q)\pi^3(n_I\rho_c^4)}{m_q^*} \frac{(3+\cos\theta)}{6(5+2\cos\theta+\cos^2\theta)} \times \left[\ln\left(c\frac{\tilde{s}}{m_g^2}\right) + \ln\left(\frac{1-\cos\theta}{1+\cos\theta}\right)\right] \tag{17}$$

where the zeroth order cross section in Eq. (8) is used for normalization.

B. SSA: experiment

To compare with the semi-inclusive data on $p_\uparrow p \to \pi X$, we set $s^\perp u(x,Q^2) = \Delta_s u(x,Q^2)$ and $s^\perp d(x,Q^2) = \Delta_s d(x,Q^2)$, with $\Delta_s u(x,Q^2)$ and $\Delta_s d(x,Q^2)$ as the spin polarized distribution functions of the valence up quarks and valence down quarks in the proton respectively. For forward π^+, π^- and π^0 productions, the SSAs are

$$A_T^{\sin\phi}(\pi^+) = \left(n_I\frac{\rho_c^4}{m_q^*}\right) k^\perp \frac{\Delta_s u(x_1,Q^2)}{u(x_1,Q^2)} \pi^3 F_g(\rho_c Q) \times \frac{(3+\cos\theta)}{6(5+2\cos\theta+\cos^2\theta)} \times \left[\ln\left(c\frac{\tilde{s}}{m_g^2}\right) + \ln\left(\frac{1-\cos\theta}{1+\cos\theta}\right)\right] \tag{18}$$

$$A_T^{\sin\phi}(\pi^-) = \left(n_I\frac{\rho_c^4}{m_q^*}\right) k^\perp \frac{\Delta_s d(x_1,Q^2)}{d(x_1,Q^2)} \pi^3 F_g(\rho_c Q) \times \frac{(3+\cos\theta)}{6(5+2\cos\theta+\cos^2\theta)} \times \left[\ln\left(c\frac{\tilde{s}}{m_g^2}\right) + \ln\left(\frac{1-\cos\theta}{1+\cos\theta}\right)\right] \tag{19}$$

$$A_T^{\sin\phi}(\pi^0) = \left(n_I\frac{\rho_c^4}{m_q^*}\right) k^\perp \frac{\Delta_s u(x_1,Q^2) + \Delta_s d(x_1,Q^2)}{u(x_1,Q^2) + d(x_1,Q^2)} \pi^3 \times F_g(\rho_c Q) \frac{(3+\cos\theta)}{6(5+2\cos\theta+\cos^2\theta)} \times \left[\ln\left(c\frac{\tilde{s}}{m_g^2}\right) + \ln\left(\frac{1-\cos\theta}{1+\cos\theta}\right)\right]. \tag{20}$$

Recently, by combining the azimuthal asymmetry in SIDIS experimental data [48,49] and $e^+e^- \to h_1 h_2 X$ data [50], the transverse distributions of up and down quarks have been extracted with Collins functions simultaneously [51–53]. Also in [54,55], the transverse distributions have been extracted by dihadron fragmentation functions (DiFFs) [56–58]. However, we note that instantons contribute to the azimuthal asymmetry in SIDIS [38–41]. Also, we will show that instantons contribute substantially to the double spin asymmetry and therefore might also contribute

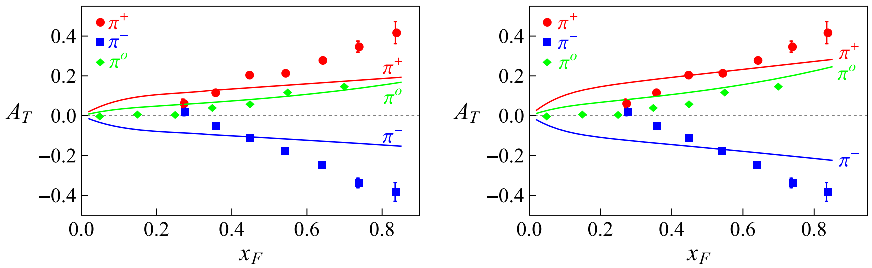

FIG. 4 (color online). x_F dependent SSA in $p_\uparrow p \to \pi X$ collisions at $\sqrt{s} = 19.$ GeV [60]. The solid lines are the analytical results in Eqs. (18)–(20) with $c = 2$ (left) and Eq. (22) (right).

largely to the $e^+e^- \to h_1 h_2 X$ process and DiFFs. It would be interesting to extract the transverse distributions of quarks in the proton by applying QCD instantons to the processes listed above. Here and for simplicity, we will estimate the SSA by using the proton helicity distributions from [59]

$$\frac{\Delta_s u(x,Q^2)}{u(x,Q^2)} = 0.959 - 0.588(1 - x^{1.048})$$
$$\frac{\Delta_s d(x,Q^2)}{d(x,Q^2)} = -0.773 + 0.478(1 - x^{1.243})$$
$$\frac{u(x,Q^2)}{d(x,Q^2)} = 0.624(1 - x). \tag{21}$$

The helicity distributions are evaluated at 1 GeV and should evolve as the scale changes. For simplicity, we ignore the effects coming from the QCD evolution and adopt the vacuum parameters of the instanton liquid model.

The results can be compared to the experimental measurements in [60]. For simplicity, we assume the same fraction for each proton $\langle x_1\rangle = \langle x_2\rangle = \langle x\rangle$, and $\langle k^\perp\rangle \approx \langle K_\perp\rangle$ is the transverse momentum of the outgoing pion. We then have $\sqrt{s}\langle x\rangle\langle\sin\theta\rangle = 2\langle K_\perp\rangle$ and $\langle x\rangle\langle\cos\theta\rangle = \langle x_F\rangle$. For large $\sqrt{s}$, we also have $\langle Q\rangle \approx \langle K_\perp\rangle\sqrt{\langle x\rangle/\langle x_F\rangle}$. We set $c = 2$ (for a best fit to π^0 data) and $\langle K_\perp\rangle = 2$ GeV for the outgoing pions. $n_I \approx 1/\mathrm{fm}^4$ is the effective instanton density, $\rho_c \approx 1/3$ fm the typical instanton size and $m_q^* \approx 300$ MeV the constitutive quark mass in the instanton vacuum. $m_g \approx 420$ MeV is the effective gluon mass in the instanton vacuum [61]. In Fig. 4 (left) we display the results (18)–(20) as a function of the parton fraction x_F for both the charged and uncharged pions at $\sqrt{s} = 19.4$ GeV [60].

Instead of isolating the collinear divergence, we can also numerically compute Eq. (9) with a massive gluon propagator as was discussed also in [42]:

$$d^{(1)}\sigma \sim i\frac{g_s^6}{(k_1 - p_1)^2 - m_g^2}\frac{1}{16\pi}\int_0^1 dy \times \int_0^{2\pi}\frac{d\phi_l}{2\pi}\frac{1}{(l_1 - k_1)^2 - m_g^2}\frac{1}{(p_1 - l_1)^2 - m_g^2}\mathcal{G}(\Omega). \tag{22}$$

The numerical results are displayed in Fig. 4 (right). Both regularizations lead about similar results. We note that our optimal choice of $c = 2$ to fit the π^0 data in Fig. 4 (left) corresponds to a gluon effective mass of about $\sqrt{c}m_g \approx 594$ MeV in the cutoff regularization (15). By choosing m_g in this range in the alternative mass regularization (22) we achieve a similar good fit to the π^0 data as well as illustrated in Fig. 4 (right), thus the consistency of the two regularizations.

In sum, the anomalous Pauli form factor can reproduce the correct magnitude of the observed SSA in polarized $p_\uparrow p \to \pi X$ for reasonable vacuum parameters. The contribution is comparable in magnitude to the one recently discussed in [41] (see Fig. 11) using instead the standard Dirac form factor but changes in the instanton distribution due to the polarized proton.

IV. DOUBLE SPIN ASYMMETRIES IN DIJET PRODUCTIONS

A. DSA: estimate

The same Pauli form factor and vacuum parameters can be used to assess the role of the QCD instantons on doubly

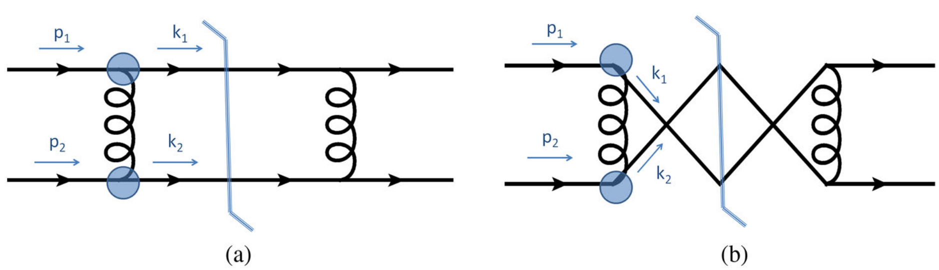

FIG. 5 (color online). The valence quark in polarized proton p_1 exchanges one gluon with the valence quark in the polarized proton p_2.

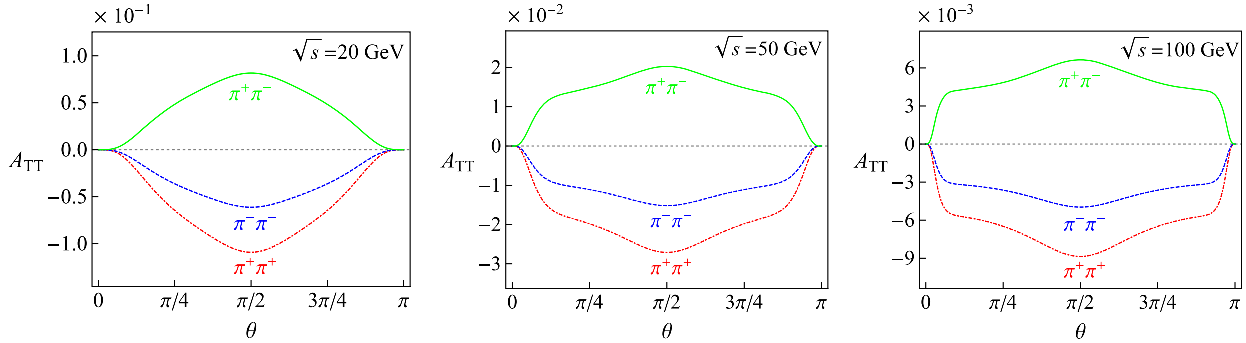

FIG. 6 (color online). Dotdashed line is the double spin asymmetry of $\pi^+\pi^+$ productions [Eq. (29)]. The dashed line is the double spin asymmetry of $\pi^-\pi^-$ productions [Eq. (30)]. The solid line is the double spin asymmetry of $\pi^+\pi^-$ productions [Eq. (31)].

polarized and semi-inclusive $p_\uparrow p_\uparrow \to \pi\pi X$ processes. The DSA is defined as

$$A_{\rm DS} = \frac{\sigma^{\uparrow\uparrow+\downarrow\downarrow} - \sigma^{\downarrow\uparrow+\uparrow\downarrow}}{\sigma^{\uparrow\uparrow+\downarrow\downarrow} + \sigma^{\downarrow\uparrow+\uparrow\downarrow}} \tag{23}$$

with the proton beam polarized along the transverse direction. The valence quark from the polarized proton P_1 exchanges one gluon with the valence quark from the polarized proton P_2 as shown in Fig. 5. At large $\sqrt{s}$, Fig. 5(a) is dominant in forward pion production and Fig. 5(b) is dominant in backward pion production. For Fig. 5(a), the differential cross section reads

$$d\sigma \sim \frac{g_s^4}{|p_1 - k_1|^4} \sum_{\rm color} {\rm tr}[M_\mu^a \not{p}_1 (1 + \gamma_5 \not{s}_1)\gamma_0 (M_\nu^b)^\dagger \gamma_0 \not{k}_1] {\rm tr}[M_\mu^a \not{p}_2 (1 + \gamma_5 \not{s}_2)\gamma_0 (M_\nu^b)^\dagger \gamma_0 \not{k}_2]. \tag{24}$$

Using the anomalous Pauli form factor (6), the contribution to the DSA follows from simple algebra

$$\begin{aligned} d^{(2)}\sigma \sim \frac{256}{|p_1 - k_1|^4} \left(\frac{F_g(\rho_c Q)\pi^4 n_I \rho_c^4}{m_q^*}\right)^2 &[(k_1 \cdot s_1)(k_1 \cdot s_2)(k_2 \cdot p_1)(k_2 \cdot p_2) - (k_1 \cdot p_1)(k_1 \cdot s_2)(k_2 \cdot p_2)(k_2 \cdot s_1) \\ &- (k_1 \cdot s_1)(k_1 \cdot s_2)(k_2 \cdot p_2)(p_1 \cdot p_2) + (k_1 \cdot k_2)(k_1 \cdot p_1)(k_2 \cdot p_2)(s_1 \cdot s_2) - (k_1 \cdot p_1)(k_1 \cdot p_2)(k_2 \cdot p_2)(s_1 \cdot s_2) \\ &- (k_1 \cdot p_1)(k_2 \cdot p_1)(k_2 \cdot p_2(s_1 \cdot s_2) + (k_1 \cdot p_1)(k_2 \cdot p_2)(p_1 \cdot p_2)(s_1 \cdot s_2) - (k_1 \cdot p_2)(k_1 \cdot s_1)(k_2 \cdot p_1)(k_2 \cdot s_2) \\ &+ (k_1 \cdot p_1)(k_1 \cdot p_2)(k_2 \cdot s_1)(k_2 \cdot s_2) + (k_1 \cdot k_2)(k_1 \cdot s_1)(k_2 \cdot s_2)(p_1 \cdot p_2) - (k_1 \cdot p_1)(k_2 \cdot s_1)(k_2 \cdot s_2)(p_1 \cdot p_2)] \end{aligned} \tag{25}$$

after using the identity

$$\begin{aligned} &{\rm tr}[(\gamma_\mu \not{q} - \not{q}\gamma_\mu)\not{p}\gamma_5 \not{s}\gamma_\nu \not{k}] + {\rm tr}[\gamma_\mu \not{p}\gamma_5 \not{s}(\not{q}\gamma_\nu - \gamma_\nu \not{q})\not{k}] \\ &= {\rm tr}[(\gamma_\mu \not{k} + \not{p}\gamma_\mu)\not{p}\gamma_5 \not{s}\gamma_\nu \not{k}] + {\rm tr}[\gamma_\mu \not{p}\gamma_5 \not{s}(\not{k}\gamma_\nu + \gamma_\nu \not{p})\not{k}] \\ &= 8i[p_\mu \epsilon(\nu, k, p, s) - p_\nu \epsilon(\mu, k, p, s) + (k \cdot p)\epsilon(\mu, \nu, k, s) - (k \cdot s)\epsilon(\mu, \nu, k, p)] \end{aligned} \tag{26}$$

where we used $q = k - p$ and $p \cdot s = 0$ because the protons are transversely polarized.

For a simple empirical application of (25) we adopt the simple kinematical setup in Eq. (12). Obtain

$$d^{(2)}\sigma \sim -\frac{4}{|p_1 - k_1|^4} \left(\frac{F_g(\rho_c Q)\pi^4 n_I \rho_c^4}{m_q^*}\right)^2 \tilde{s}^3 s_1^\perp s_2^\perp (1 - \cos\theta)^2 [4 + \cos(\theta - 2\phi) + 2\cos(2\phi) + \cos(\theta + 2\phi)]. \tag{27}$$

After adding the contribution of Figs. 5(a)–5(b), and averaging over the transverse direction ϕ, we finally obtain

$$\frac{d^{(2)}\sigma}{d^{(0)}\sigma} \sim -4 s_1^\perp s_2^\perp \left(\frac{\pi^4 n_I \rho_c^4}{m_q^* g_s^2}\right)^2 \frac{F_g^2\left[\rho_c \sqrt{\frac{\tilde{s}(1-\cos\theta)}{2}}\right]\tilde{s} + F_g^2\left[\rho_c \sqrt{\frac{\tilde{s}(1+\cos\theta)}{2}}\right]\tilde{s}}{\frac{5+2\cos\theta+\cos^2\theta}{(1-\cos\theta)^2} + \frac{5-2\cos\theta+\cos^2\theta}{(1+\cos\theta)^2}}. \tag{28}$$

B. DSA: results

Our DSA results can now be compared to future experiments at collider energies. Specifically, our DSA for dijet productions is

$$A_{\pi^+\pi^+} = -\frac{1}{8}\frac{\Delta_s u(x_1,Q^2)}{u(x_1,Q^2)}\frac{\Delta_s u(x_2,Q^2)}{u(x_2,Q^2)}\left(\frac{\pi^3 n_I \rho_c^4}{m_q^* \alpha_s}\right)^2 \frac{F_g^2\left[\rho_c\sqrt{\frac{\tilde{s}(1-\cos\theta)}{2}}\right]\tilde{s} + F_g^2\left[\rho_c\sqrt{\frac{\tilde{s}(1+\cos\theta)}{2}}\right]\tilde{s}}{(5+10\cos^2\theta+\cos^4\theta)\csc^4\theta} \tag{29}$$

$$A_{\pi^-\pi^-} = -\frac{1}{8}\frac{\Delta_s d(x_1,Q^2)}{d(x_1,Q^2)}\frac{\Delta_s d(x_2,Q^2)}{d(x_2,Q^2)}\left(\frac{\pi^3 n_I \rho_c^4}{m_q^* \alpha_s}\right)^2 \frac{F_g^2\left[\rho_c\sqrt{\frac{\tilde{s}(1-\cos\theta)}{2}}\right]\tilde{s} + F_g^2\left[\rho_c\sqrt{\frac{\tilde{s}(1+\cos\theta)}{2}}\right]\tilde{s}}{(5+10\cos^2\theta+\cos^4\theta)\csc^4\theta} \tag{30}$$

$$A_{\pi^+\pi^-} = -\frac{1}{8}\frac{\Delta_s u(x_1,Q^2)\Delta_s d(x_2,Q^2)+\Delta_s d(x_1,Q^2)\Delta_s u(x_2,Q^2)}{u(x_1,Q^2)d(x_2,Q^2)+d(x_1,Q^2)u(x_2,Q^2)}\left(\frac{\pi^3 n_I \rho_c^4}{m_q^* \alpha_s}\right)^2 \frac{F_g^2\left[\rho_c\sqrt{\frac{\tilde{s}(1-\cos\theta)}{2}}\right]\tilde{s} + F_g^2\left[\rho_c\sqrt{\frac{\tilde{s}(1+\cos\theta)}{2}}\right]\tilde{s}}{(5+10\cos^2\theta+\cos^4\theta)\csc^4\theta}. \tag{31}$$

We will assume that each parton carries one third of the momentum of the proton $\langle x_1\rangle = \langle x_2\rangle = 1/3$, so that $\sqrt{\tilde{s}} = \sqrt{s}/3$, where $\sqrt{s}$ is the total energy of the colliding protons. We will use the value of α_s from [62]. The instanton size is set to $1/3$ fm, density $n_I = 1/\mathrm{fm}^4$ and $m_q^* = 300$ MeV as for the SSA reviewed above. Our predictions for charged dijet production in semi-inclusive DSA are displayed in Fig. 6. We note that at $\sqrt{s}\to\infty$, the double spin asymmetries in Eqs. (29)–(31) vanish.

Our analysis uses simple kinematics and proton helicity distributions for DSA. A better analysis could be sought by extracting the transverse distributions of the quarks in the proton, using the QCD instantons contributions to the combined polarized SIDIS experiments and the $e^+e^-\to h_1 h_2 X$ processes.

V. CONCLUSIONS

QCD instantons provide a natural mechanism for large spin asymmetries in polarized dilepton and hadron scattering at collider energies. A simple mechanism for these large spin asymmetries was noted by Kochelev [38] in the form of a large Pauli form factor for a constituent quark whether through photon exchange or gluon exchange. A simple estimate of the SSA in $p_\uparrow p\to\pi X$ production compares fairly to the measured charged asymmetries in [63] both in sign and magnitude, using the instanton vacuum parameters. We have argued that the same anomalously large Pauli form factor yields substantial DSA in $p_\uparrow p_\uparrow\to\pi\pi X$. We welcome future measurements of these asymmetries at collider facilities.

ACKNOWLEDGEMENTS

This work was supported in parts by the U.S. DOE Award No. DE-FG-88ER40388.

[1] T. Schfer and E. V. Shuryak, Rev. Mod. Phys. **70**, 323 (1998).
[2] M. Nowak, M. Rho, and I. Zahed, *Chiral Nuclear Dynamics* (World Scientific, Singapore, 1996), vol. 1.
[3] E. Shuryak and I. Zahed, Phys. Rev. D **62**, 085014 (2000).
[4] M. A. Nowak, E. V. Shuryak, and I. Zahed, Phys. Rev. D **64**, 034008 (2001).
[5] E. V. Shuryak and I. Zahed, Phys. Rev. D **69**, 046005 (2004).
[6] D. Kharzeev and E. Levin, Nucl. Phys. **B578**, 351 (2000).
[7] A. Dorokhov and I. Cherednikov, Nucl. Phys. B, Proc. Suppl. **146**, 140 (2005).
[8] A. Ringwald and F. Schrempp, Phys. Lett. B **503**, 331 (2001).
[9] F. Schrempp and A. Utermann, arXiv:astro-ph/0301177.
[10] M. Giordano and E. Meggiolaro, Phys. Rev. D **81**, 074022 (2010).
[11] M. Giordano and E. Meggiolaro, *Proc. Sci.*, LATTICE2011 (2011) 155 [arXiv:1110.5188].
[12] A. Airapetian *et al.* (HERMES Collaboration), Phys. Rev. Lett. **84**, 4047 (2000).
[13] A. Airapetian *et al.* (HERMES Collaboration), Phys. Rev. Lett. **94**, 012002 (2005).

[14] A. Airapetian *et al.* (HERMES Collaboration), Phys. Rev. Lett. **103**, 152002 (2009).
[15] H. Avakian *et al.* (CLAS Collaboration), Phys. Rev. Lett. **105**, 262002 (2010).
[16] M. Alekseev *et al.* (COMPASS Collaboration), Phys. Lett. B **692**, 240 (2010).
[17] M. Alekseev *et al.* (COMPASS Collaboration), Phys. Lett. B **673**, 127 (2009).
[18] B. I. Abelev *et al.* (STAR Collaboration), Phys. Rev. Lett. **101**, 222001 (2008).
[19] K. Eyser (PHENIX Collaboration), AIP Conf. Proc. **842**, 404 (2006).
[20] D. Adams *et al.* (FNAL E704 Collaboration), Phys. Lett. B **264**, 462 (1991).
[21] D. Sivers, Phys. Rev. D **41**, 83 (1990).
[22] D. Sivers, Phys. Rev. D **43**, 261 (1991).
[23] J. Collins, Nucl. Phys. **B396**, 161 (1993).
[24] J. Collins, S. Heppelmann, and G. Ladinsky, Nucl. Phys. **B420**, 565 (1994).
[25] D. Amrath, A. Bacchetta, and A. Metz, Phys. Rev. D **71**, 114018 (2005).
[26] A. Bacchetta, L. P. Gamberg, G. R. Goldstein, and A. Mukherjee, Phys. Lett. B **659**, 234 (2008).
[27] S. J. Brodsky, D. S. Hwang, and I. Schmidt, Phys. Lett. B **530**, 99 (2002).
[28] D. Boer, S. J. Brodsky, and D. S. Hwang, Phys. Rev. D **67**, 054003 (2003).
[29] S. Meissner, A. Metz, and K. Goeke, Phys. Rev. D **76**, 034002 (2007).
[30] A. Bacchetta, F. Conti, and M. Radici, Phys. Rev. D **78**, 074010 (2008).
[31] L. P. Gamberg, G. R. Goldstein, and M. Schlegel, Phys. Rev. D **77**, 094016 (2008).
[32] Z. Lu, B.-Q. Ma, and J. She, Phys. Lett. B **696**, 513 (2011).
[33] F. Yuan, Phys. Lett. B **575**, 45 (2003).
[34] I. Cherednikov, U. D'Alesio, N. Kochelev, and F. Murgia, Phys. Lett. B **642**, 39 (2006).
[35] A. Courtoy, F. Fratini, S. Scopetta, and V. Vento, Phys. Rev. D **78**, 034002 (2008).
[36] S. J. Brodsky, B. Pasquini, B.-W. Xiao, and F. Yuan, Phys. Lett. B **687**, 327 (2010).
[37] B. Pasquini and P. Schweitzer, Phys. Rev. D **83**, 114044 (2011).
[38] N. Kochelev, JETP Lett. **72**, 481 (2000).
[39] A. Dorokhov, N. Kochelev, and W. Nowak, Phys. Part. Nucl. Lett. **6**, 440 (2009).
[40] D. Ostrovsky and E. Shuryak, Phys. Rev. D **71**, 014037 (2005).
[41] Y. Qian and I. Zahed, Phys. Rev. D **86**, 014033 (2012).
[42] N. Kochelev and N. Korchagin, Phys. Lett. B **729**, 117 (2014).
[43] G. 't Hooft, Phys. Rev. D **14**, 3432 (1976).
[44] A. Vainshtein, V. I. Zakharov, V. Novikov, and M. A. Shifman, Sov. Phys. Usp. **25**, 195 (1982).
[45] N. Kochelev, Phys. Lett. B **426**, 149 (1998).
[46] E. V. Shuryak, Nucl. Phys. **B198**, 83 (1982).
[47] B. Potter Theoretische Elementarteilchenphysik, Hamburg University (1997).
[48] A. Airapetian *et al.* (HERMES Collaboration), Phys. Rev. Lett. **94**, 012002 (2005).
[49] E. Ageev *et al.* (COMPASS Collaboration), Nucl. Phys. **B765**, 31 (2007).
[50] K. Abe *et al.* (Belle Collaboration), Phys. Rev. Lett. **96**, 232002 (2006).
[51] M. Anselmino, M. Boglione, U. D'Alesio, A. Kotzinian, F. Murgia, A. Prokudin, and C. Türk, Phys. Rev. D **75**, 054032 (2007).
[52] M. Anselmino, M. Boglione, U. D'Alesio, S. Melis, F. Murgia, and A. Prokudin, Phys. Rev. D **87**, 094019 (2013).
[53] M. Anselmino, M. Boglione, U. D'Alesio, A. Kotzinian, F. Murgia, A. Prokudin, and S. Melis, Nucl. Phys. B, Proc. Suppl. **191**, 98 (2009).
[54] A. Bacchetta, A. Courtoy, and M. Radici, J. High Energy Phys. 03 (2013) 119.
[55] M. Radici, A. Courtoy, and A. Bacchetta, in *The Proceedings of the 4th International Workshop on Transverse Polarization Phenomena in Hard Processes, Italy, 2014*.
[56] J. C. Collins, S. F. Heppelmann, and G. A. Ladinsky, Nucl. Phys. **B420**, 565 (1994).
[57] R. Jaffe, X.-m. Jin, and J. Tang, Phys. Rev. Lett. **80**, 1166 (1998).
[58] M. Radici, R. Jakob, and A. Bianconi, Phys. Rev. D **65**, 074031 (2002).
[59] M. Hirai, S. Kumano, and N. Saito, Phys. Rev. D **74**, 014015 (2006).
[60] D. Adams *et al.* (Fermilab E704 Collaboration), Nucl. Phys. **B510**, 3 (1998).
[61] M. Hutter, arXiv:hep-ph/9501335.
[62] J. Beringer *et al.* (Particle Data Group), Phys. Rev. D **86**, 010001 (2012).
[63] J. Skeens (E704 Collaboration), AIP Conf. Proc. **243**, 1008 (1992).